

Analysis of TRPC3-Interacting Proteins by Tandem Mass Spectrometry

Timothy Lockwich,[†] Jaya Pant,[‡] Anthony Makusky,[‡] Ewa Jankowska-Stephens,[‡]
 Jeffrey A. Kowalak,[‡] Sanford P. Markey,^{*,†} and Indu S. Ambudkar^{*,†}

Secretary Physiology Section, Molecular Physiology and Therapeutics Branch, NIDCR, National Institutes of Health, Bethesda, Maryland 20892, and Laboratory of Neurotoxicology, National Institute of Mental Health, National Institutes of Health, Bethesda, Maryland 20892

Received August 2, 2007

Mammalian transient receptor potential canonical (TRPC) channels are a family of nonspecific cation channels that are activated in response to stimulation of phospholipase C (PLC)-dependent hydrolysis of the membrane lipid phosphatidylinositol 4,5-bisphosphate. Despite extensive studies, the mechanism(s) involved in regulation of mammalian TRPC channels remains unknown. Presence of various protein-interacting domains in TRPC channels have led to the suggestion that they associate with proteins that are involved in their function and regulation. This study was directed toward identifying the proteins associated with native TRPC3 using a shotgun proteomic approach. Anti-TRPC3 antibody was used to immunoprecipitate TRPC3 from solubilized rat brain crude membranes under conditions that allow retention of TRPC3 function. Proteins in the TRPC3 (using anti-TRPC3 antibody) and control (using rabbit IgG) immunoprecipitates were separated by SDS-PAGE, the gel was sectioned, and the resolved proteins were digested by trypsin *in situ*. After extraction of the peptides, the peptides were separated by HPLC and sequences derived by MS/MS. Analysis of the data revealed 64 specific TRPC3-associated proteins which can be grouped in terms of their cellular location and involvement in specific cellular function. Many of the proteins identified have been previously reported as TRPC3-regulatory proteins, such as IP₃Rs and vesicle trafficking proteins. In addition, we report novel putative TRPC3-interacting proteins, including those involved in protein endocytosis and neuronal growth. To our knowledge, this is the first comprehensive proteomic analysis of a native TRPC channel. These data reveal potential TRPC3 regulatory proteins and provide novel insights of the mechanism(s) regulating TRPC3 channels as well as the possible cellular functions where the channel might be involved.

Keywords: proteomic analysis • TRPC3 • protein complex • signaling

Introduction

The mammalian transient receptor potential canonical (TRPC) cation channels are a family of nonselective cation channels that are activated in response to stimulation of G-protein-coupled receptors linked to phosphatidylinositol 4,5-bisphosphate (PIP₂) hydrolysis in a variety of tissues. Although the exact nature of mammalian TRPC channel activation is still unknown, studies with the TRP channel "signalplex" in the *Drosophila* phototransduction cascade reveal that the TRP channel resides in a complex where both TRP-TRP interactions and TRP interactions with other proteins in the signaling complex are important for proper channel activity and regula-

tion.¹ Consistent with the *Drosophila* model, studies of mammalian TRPC channels (which share significant structural similarities to the *Drosophila* TRP channel) also reveal an extensive network of interactions between TRPC monomers as well as between TRPCs and other proteins.² It is now evident that the protein-protein interactions of the mammalian TRPC channels are crucial for the proper function and regulation of mammalian TRPC channel activity.¹⁻⁴ There are convincing data to show that some TRPC members are dynamically regulated. TRPC3, TRPC5, and TRPC6 are localized intracellularly in mobile vesicles that are recruited to the plasma membrane following cell stimulation.³ We have previously reported that TRPC3 is physically translocated from intracellular membrane systems to the plasma membrane upon activation via a vesicle fusion mechanism that involves members of the SNARE complex that mediates vesicle exocytosis.⁵ Clearly, these changes in the protein-protein interactions as TRPC channels undergo activation need to be elucidated in order to define the exact molecular mechanisms by which the channels are regulated. However, a comprehensive analysis of proteins interacting with native TRPC channels is lacking.

* To whom correspondence should be addressed. Dr. Sanford P. Markey, 10 Center Drive, Bldg 10, Room 3D42, Bethesda, MD 20892. Phone: 301-496-5298. Fax: 301-451-5780. E-mail: markeys@mail.nih.gov. Dr. Indu S. Ambudkar, Bldg. 10, Room 1N-113, NIH, Bethesda, MD 20894. Phone: 301-496-5298. Fax: 301-428-1228. E-mail: indu.ambudkar@nih.gov.

[†] Secretary Physiology Section, Molecular Physiology and Therapeutics Branch, NIDCR, National Institutes of Health.

[‡] Laboratory of Neurotoxicology, National Institute of Mental Health, National Institutes of Health.

Complicating this undertaking are the extensive interactions that the TRP proteins have with other organelles and structures within the cell. Various TRPC family members have been shown to reside in lipid raft domains,⁶ interact with endoplasmic reticulum (ER),⁷ interact with cytoskeletal scaffolding structures,¹ and co-localize with a subpopulation of mitochondria (peripheral) located near the plasma membrane.⁸

Attempts to elucidate the protein-protein interactions in TRPC channel complexes have utilized techniques such as co-immunoprecipitation, co-localization, GST-fusion protein interactions, and yeast two-hybrid analysis. Such approaches have revealed a variety of signaling, trafficking, and scaffolding proteins that functionally interact with TRPC channels.² However, there are limitations inherent in each of these methods. For example, the use of tagged, overexpressed proteins can yield unnatural interactions, and the non-native environment in yeast two-hybrid analysis suffers from the same shortcoming. Further, these approaches, with the exception of a yeast two-hybrid screen of a cDNA library, are largely "hypothesis driven", in which candidate proteins are selected based on functional data or cellular localization and then screened for interactions.

To obtain a more comprehensive and unbiased survey of interacting proteins, we have used a shotgun proteomic approach on a native TRPC channel (TRPC3 in rat brain). As reported in several previous studies, TRPC3 is highly expressed in brain.⁹ This study uses an anti-TRPC3 antibody to immunoprecipitate native TRPC3 protein from solubilized rat brain crude membranes under relatively stringent conditions. The immunoprecipitate was subjected to SDS-PAGE, and the resultant gel slices were treated with trypsin. After extraction of the peptides, the mixture was separated using HPLC, and peptide sequences were derived from tandem mass spectrometry (MS/MS). To our knowledge, this report represents the first shotgun proteomic analysis of a native TRPC protein. While our results confirm many previously reported accessory proteins for TRPC3, we also report several novel proteins as well as regulatory pathways that are potentially critical in regulating the assembly and function of these channels as well as in mediating the effects of TRPC3 on neuronal function.

Experimental Procedures

Antibodies and Reagents. Anti-TRPC3 was a generous gift from Dr. Randen Patterson and has been described before.¹⁰ Commercial antibodies used were from the following sources: rabbit anti-IgG, anti-GAP-43 (neuromodulin), anti-clathrin heavy chain, and anti-adenine nucleotide translocator 1 (ANT1) were from Santa Cruz Biotechnology (Santa Cruz, CA). Anti-Na⁺/K⁺-ATPase, FLAG peptide, and anti-FLAG M2-agarose from mouse were from Sigma (St. Louis, MO). Sequencing grade modified trypsin was from Promega (Madison, WI). *Escherichia coli* washed lipids, phosphatidylethanolamine (PE), phosphatidylcholine (PC), and cholesterol were from Avanti Polar Lipids (Alabaster, AL), and *n*-octyl- β -D-glucopyranoside (octylglucoside) was from Calbiochem (La Jolla, CA). 4-(2-Aminoethyl)-benzene-sulfonyl fluoride hydrochloride (AEBSF) was from MP Biomedicals (Solon, OH). 1-Oleoyl-2 acetyl-*sn*-glycerol (OAG) was from Calbiochem (San Diego, CA). All other reagents were reagent grade from Sigma (St. Louis, MO) except for dithiothreitol (DTT), which was Sigma UltraGrade.

Preparation of Crude Membranes. (All steps were done at 4 °C.) Frozen rat brains (Taconic Farms, Hudson, NY) were thawed in ice-cold homogenization buffer consisting of 0.25 M sucrose, 10 mM TRIS-HEPES (pH 7.4), 0.1 mM phenylm-

ethylsulfonyl fluoride (PMSF), and 1 mM DTT. After thawing, the brains were washed 3 times (~20 mL per brain) to remove hair and blood. Each washed brain was homogenized in a Kontes hand-held homogenizer 30 times with both pestles in 15 mL of homogenization buffer. The homogenate was transferred into a Beckman JA-20 centrifuge tube, diluted to 30 mL using homogenization buffer, then spun at 3000g for 15 min to remove cell debris. The supernatant was filtered through 4 layers of cheesecloth and spun again at 23,500g. The pellet was resuspended in homogenization buffer to a protein concentration of 10–15 mg/mL (as determined by BioRad Protein Assay, Hercules, CA). The resuspended pellet was then aliquoted and stored at -70 °C until further use.

Solubilization and Immunoprecipitation. (All steps were done at 4 °C.) Five milligrams of crude membranes (prepared as described above) was diluted into 5–6 mL of a repelling buffer consisting of 200 mM KCl, 50 mM K-MOPS (pH 7.5), 2.5 mM MgCl₂, 1 mM DTT, 2 μ g/mL of leupeptin and pepstatin A, and 0.5 mM AEBSF and spun at 60,000g for 15 min. The supernatant was discarded and the pellet resuspended in 2.4 mL of a solubilization media consisting of 50 mM K-MOPS (pH 7.5), 1.5% octylglucoside, 0.5 M KI, 20% glycerol, 200 μ L of a 50 mg/mL lipid stock (in 2 mM β -mercaptoethanol consisting of washed *E. coli* lipids/PC/PS/cholesterol in a ratio (w/w) of 60/17.5/10/12.5), 1.5 mM MgCl₂, 1 mM DTT, 0.5 mM AEBSF, and 2 μ g/mL of leupeptin and pepstatin A. The mixture was kept on ice for 20 min, then centrifuged for 1 h at 145,000g. The supernatant (octylglucoside extract) was used for immunoprecipitation experiments. For immunoprecipitation, 50 mg of Protein A Sepharose CL-4B beads (Amersham, Uppsala, Sweden) were washed three times with 1 mL of TBS buffer (50 mM Tris HCl and 150 mM NaCl, pH 7.4) by rotating wheel for 5 min, then spun for 1 min at 1000g (all subsequent spins involving the immunoprecipitation procedure were done using these parameters). The beads were washed once with 1 mL of the solubilization media (without protein) for 5 min before centrifugation to allow removal of the wash. A slurry was made with the washed beads by adding 150 μ L of solubilization media (without protein), and 50 μ L of this slurry was added to 1 mL of the octylglucoside extract to prewash the extract and equilibrated for 30 min using a rotating wheel. After centrifugation, the prewashed extract was transferred to a new tube and mixed with either 2 μ g of rabbit IgG (Santa Cruz Biotechnology, Santa Cruz, CA) or 25 μ L of a rabbit IgG directed against TRPC3 (as described previously) for 1 h using a rotary wheel. The extract/IgG mixtures were transferred to the remaining Protein A Sepharose CL-4B beads (after removing the remaining solubilization media). The combined extract/IgG/bead mixture was equilibrated overnight using a rotating wheel. The non-binding fraction was removed after centrifugation, and the beads were washed (3 \times , 5 min each) with 1 mL of a buffer containing 500 mM NaCl, 10 mM Tris-Cl (pH 7.5), 1 mM ethylenediaminetetraacetic acid (EDTA), 0.2 mM sodium vanadate, 0.2 mM PMSF, 0.5% Nonidet P-40, 10% sucrose, and 1 μ g/mL aprotinin, leupeptin, and pepstatin A. The antibody-selected proteins were then eluted from the beads using 100 μ L of a 2 \times NuPAGE LDS Sample buffer (Invitrogen, Carlsbad, CA) enhanced with 200 mM DTT by boiling for 5 min, then separated from the beads by centrifuging with 0.45 μ m Ultrafree-MC centrifugal device (Millipore, Bedford, MA) for 3 min at 1000g. Typically, 300 μ L of the separated proteins in sample buffer were then concentrated to 80–100 μ L using Microcon YM-10 centrifugal devices (Millipore) before SDS-PAGE.

A similar solubilization and immunoprecipitation of FLAG-TRPC3 or FLAG-mut TRPC3 (where LFW residues in the proposed pore region between the fifth and sixth transmembrane regions were changed to alanine),¹¹ from plasma membrane fractions of stably transfected HEK-293 cells (plasma membrane preparation was described previously¹²), was performed to gauge Ca^{2+} transport activity in proteoliposomes. In these immunoprecipitations, all steps were identical except for the following: extracts from the control HEK, FLAG-TRPC3, and FLAG-mut TRPC3 membranes were not prewashed but rather applied directly to 200 μL of ANTI-FLAG M2 Affinity Gel (Sigma Chemical Co., St. Louis, MO) and subsequently released by equilibrating with 2 mM free FLAG peptide for 2 h at 4 °C. The resultant IP fraction was not concentrated before incorporation into proteoliposomes.

Reconstitution and $^{45}\text{Ca}^{2+}$ Flux Assays of Immunoprecipitated FLAG-Tagged Proteins. A total of 300 μL of the IP fraction from either HEK solubilized membranes (control), FLAG-TRPC3 HEK, or FLAG-mut TRPC3 solubilized membranes was mixed on ice with 2.6 mL of a dilution buffer identical to the extraction buffer described above (but without KI and lipids) and 100 μL of a lipid preparation (9:1 50 mg/mL lipid solution/1 M Tris-HCl, pH 7.4) sonicated until clarity. This solution was injected into a 3–15 mL 10K molecular weight cutoff Slide-A-Lyzer (Pierce, Rockford, IL) and dialyzed three times for 20 min against 300 mL of a dialysis buffer consisting of 50 mM Tris-HCl, pH 7.4, 1% (v/v) of a 1.7 mg/mL aprotinin solution (Sigma), and 1 mM DTT. The dialysate was removed from the Slide-A-Lyzer and centrifuged for 40 min at 150,000g. The resultant pellet containing the proteoliposomes was re-suspended in 100 μL of a resuspension/assay/wash buffer consisting of 50 mM K-MOPS, pH 7.4, 200 mM KCl, 1 mM MgCl₂, and 1 mM DTT using a 25 gauge needle. The $^{45}\text{Ca}^{2+}$ flux assays were initiated at 37 °C by introducing 10% (v/v) proteoliposomes into resuspension/assay/wash media containing either 25 μM or 1 mM $^{45}\text{CaCl}_2$. After 20, 40, and 60 s, 100 μL aliquots were filtered through Millipore filters (0.22 μm , type GSWP) using a Millipore filtration system and washed three times with 3 mL of ice-cold resuspension/assay/wash media. The filters were air-dried and counted for radioactivity in a scintillation counter. In some experiments, HEK and FLAG TRPC3 proteoliposomes were added to 1 mM $^{45}\text{CaCl}_2$ equilibrated with 50 μM of OAG (a diacylglycerol analogue) for 20 s before filtration.

Validation by Western Blot Co-immunoprecipitation. To confirm MS/MS identification, Western blots were performed on 35 μL of the TRPC3 IP fraction (not concentrated) using the native antibody. For MS/MS identifications involving proteins only detected in the TRPC3 IP fraction (and not the control IgG IP fraction), the antibody against the TRPC3-interacting protein was used to confirm the presence of the protein in the TRPC3 immunocomplex. To confirm the quantitative differences of proteins detected in both the TRPC3 and control IgG immunocomplexes, equal amounts of IP fractions (as determined by density scanning of the heavy and light chains of the IgG after silver staining of the SDS-PAGE gel, Silver SNAP Stain II Kit, Pierce Biotechnology, Inc., Rockford, IL) were probed with the antibody of the suspected interacting protein and quantitatively analyzed using a Bio-Rad Eagle Eye digital scanning device. Candidates for quantitative confirmation were initially identified by at least a 2-fold increase in the amplitude of the common peptides in the TRPC3 IP by MS (in full-scan mode).

SDS-PAGE and In-Gel Trypsin Digestion. Fifty microliters of the released, concentrated proteins was loaded onto Nu-PAGE 8% Bis-Tris Gels (Invitrogen, Carlsbad, CA). After electrophoresis, the gel was stained overnight in 0.1% Coomassie R250, 20% methanol, and 0.5% acetic acid. The gels were destained using 30% methanol until the protein bands were visible and the background nearly clear. The gel lanes were sliced into ~40 vertical slices (1.5 mm) and placed into individual tubes. The gel slices were washed for 1 h in 100 mM ammonium bicarbonate, and the wash was discarded. A total of 150 μL of 100 mM ammonium bicarbonate was added followed by the addition of 10 μL of 45 mM DTT. The tubes were incubated at 60 °C for 30 min, then cooled to room temperature. Ten microliters of 100 mM iodoacetamide was then added to each tube and incubated in the dark with gentle shaking for 30 min. The solvent was removed, and the gel slices were equilibrated with 500 μL of 50% acetonitrile/50 mM ammonium bicarbonate for 1 h with gentle shaking. After the solvent was removed, each gel slice was cut into 2–3 pieces, and 50 μL of acetonitrile was added and equilibrated for 15 min. The solvent was removed, and the gel slices were dried using a rotary evaporator. Ten microliters of a solution consisting of 0.02 $\mu\text{g}/\mu\text{L}$ modified trypsin (Promega, Madison, WI) in 25 mM ammonium bicarbonate was then added and absorbed into the dried gel slices. After 15 min, additional 25 mM ammonium bicarbonate was added to cover the cover slices and the digest allowed to proceed overnight at 37 °C with gentle shaking. The digestion media was transferred to a new tube, and 25 μL of a solution consisting of 50% acetonitrile and 0.1% trifluoroacetic acid (TFA) was added to the gel slices. After sonication in a water bath type sonicator for 20 min, the extract was added to the original digestion media, and the gel slices were re-extracted with 25 μL of a solution containing 80% acetonitrile and 0.1% TFA by sonicating for 20 min. The re-extraction media was pooled with the digestion and extraction media and dried using a rotary evaporator.

Automated 1D LC-MS/MS. The fully automated nanoflow 1D HPLC system has been described in detail elsewhere.¹³ Briefly, 1D HPLC system was built using LC-VP Series components, consisting of an SCL-10AVP controller, a DGU-14A online degasser, three LC-10ADVP pumps with microflow control firmware, an SIL-10ADVP autosampler, and an SCL-10AVP system controller (Shimadzu Corporation, Kyoto, Japan). A Peptide CapTrap (0.5 mm \times 2 mm i.d., 0.5 μL bed volume; Michrom BioResource Inc., Auburn, CA) mounted on a 2-position, 6-port Cheminert nanovolume valve (Model CN2; Valco Instruments Co., Houston, TX) was used as trapping column for trapping, desalting, and loading samples onto the capillary reversed-phase column. Nanoflow chromatography was achieved using a flow splitting device consisting of a pressure regulator (Upchurch Scientific, Oak Harbor, WA) and a T-joint with the pump flow rate at 15 $\mu\text{L}/\text{min}$. The HPLC column was an uncoated PicoFrit capillary column (Betabasic C18 resin, 5 μm particle size, 10 cm bed volume, 360 μm o.d., 75 μm i.d., 15 μm orifice; New Objective, Inc., Woburn, MA) which was interfaced through a New Objective PicoView ESI Source (Woburn, MA) directly into a ThermoFinnigan LCQ Classic ESI-ion trap mass spectrometer (San Jose, CA). The autosampler was used to inject samples onto the trapping column. Peptides on the CapTrap were desalted using RP-C at 40 $\mu\text{L}/\text{min}$ for 3 min and then eluted sequentially onto the RP column and into the mass spectrometer using the following elution program:

10% B (isocratic flow for 3 min), a linear gradient of 10–60% B (40 min), 60–80% B (5 min), 80% B (2 min) at 400 nL/min. Mobile phase buffers were RP-A, water/ acetonitrile/formic acid, 94.9/5/0.1 (v/v/v); RP-B, water/ acetonitrile/formic acid, 19.9/80/0.1 (v/v/v); and for RP-C, water/formic acid, 99.9/0.1 (v/v). The RP mixer volume was 2 μ L. The LCQ was operated in positive ion mode with dynamic exclusion set to repeat count = 3, repeat duration = 0.50 min, exclusion duration = 0.5 min, exclusion mass width = 3 amu. Centroided spectra were acquired in a data-dependent manner with the top three most intense ions in the full MS scan selected for MS/MS. Data-dependent parameters were normalized collision energy = 35%, default charge state = 3, min MS signal intensity = 5×10^5 (nominally S/N = 5 based on baseline chemical noise under equilibrium LC conditions at 10% B), and isolation width = 4 amu.

Database Searching and Data Processing. MS/MS spectral data were processed for automated interpretation using Mascot Daemon (version 2.1, Matrix Science Ltd., London, U.K.). Briefly, the Mascot Daemon uses a program (LCQ_DTA.exe) to extract peak lists (*m/z* versus intensity pairs) for each MS/MS spectrum in a given data file, and concatenates these peak lists into one composite file. Parameters used for peak list extraction were minimum mass = 400, maximum mass = 4000, group tolerance = 1.4 Da, intermediate scans = 0, minimum scans/group = 1, and precursor charge state = auto. After peak list generation, Mascot Daemon transfers the data and a user-specified set of search parameters to the Mascot search engine¹⁴ (version 2.1, Matrix Science Ltd., London, U.K.). Mascot was configured to search the UniProtKB/Swiss-Prot Release 51.2 database (12.06.2006)¹⁵ using “*Rattus*” as a taxonomic restrictor. Other user defined parameters were enzyme = trypsin, fixed modifications = carbamidomethylation of Cys, variable modification = oxidation of Met, precursor ion mass tolerance = 2.0 Da, product ion mass tolerance = 0.8 Da, possible charge states = +1, +2, and +3, and use monoisotopic mass values was specified. The information contained in individual Mascot reports was parsed into a relational database using the software DBParser.¹⁶ Mascot produces probability based scores with a significance threshold of $p < 0.05$. Peptide identifications were accepted if the Mascot Ions Score exceeded the database-dependent Identity Score. DBParser facilitated the concatenation of multiple data sets, and afforded multiple data set comparisons, and generated context-specific reports, for example, a parsimonious list of proteins present based on unique peptides in each data set.

Details of Quantification. The utilities of DBParser have been extended to include metasearching (multiple search engine comparisons, i.e., Mascot, OMSSA and X! Tandem) and ion-current based quantification.¹⁷ The stability of LC–MS/MS ion current makes it useful to retrieve label-free quantitative information such as retention time, peak intensity, and integrated area which affords the ability to compare the same putative precursor protein between experiments. For quantification, DBParser extracts retention time and peak intensity from raw data based on the precursor mass identified by Mascot. The peak area and number of scans are then calculated from the selected ion chromatogram. Mass tolerance for extraction of ion current is user-selected and instrument-dependent. In the case of the LCQ classic employed here, a mass tolerance of ± 0.6 Da was used. In addition to peptide sequence, *m/z*, Ions Score, Homology Score, and Identity Score from Mascot search, quantification reports include retention

time, peak intensity, area, and number of scans. Quantitative differences of the same protein identified in both the control and TRPC3 samples were analyzed by comparing the sum intensity ratio (TRPC3/control) of a unique peptide present in both runs (when possible). If a quantitative ratio of $>2\times$ resulted, we interpreted this difference as a quantitative difference and not resulting from a mere nonspecific binding event. When possible, Western blot analysis of equal amounts of control-IP and TRPC3-IP fractions were analyzed to confirm quantitative differences. To analyze family of proteins, cluster analysis of shared peptides was performed using MassSieve¹⁸ in order to determine if unique sequences were present in individual family members. Only family members with at least one unique sequence were included into the “specific TRPC3 interacting protein” category.

Cluster Analysis using MassSieve. Because of rapid expansion in the size of MS/MS data sets and the equally rapid expansion of protein sequence libraries, we have determined that the structure of DBParser is limiting. A new program, MassSieve¹⁸ is being developed that is scalable and not sensitive to file size limitations. Important benefits of this effort are improved speed of the algorithm and a more facile and interactive user interface. MassSieve includes a graphical display of peptide–protein relations for visualization of peptides shared between possible protein isoforms and is particularly useful for reconciling discrepancies in quantification ratios for different peptides in the same putative protein. Additionally, MassSieve allows access to all relevant metrics required needed to comply with reporting guidelines stipulated by proteomics journals.

Results

Immunoprecipitated TRPC3 Mediates Ca^{2+} Flux after Reconstitution into Proteoliposomes. To obtain a functionally relevant preparation of TRPC3, we assessed the ability of solubilized and immunoprecipitated FLAG-TRPC3 to mediate $^{45}\text{Ca}^{2+}$ flux following reconstitution into proteoliposomes (PrL). The immunoprecipitated (IP) fractions from control HEK and FLAG-TRPC3-expressing HEK-293 cells were reconstituted as described in Experimental Procedures. Figure 1A shows the presence of FLAG-TRPC3 in the proteoliposomes prepared from FLAG-TRPC3-expressing HEK-293 cells and the absence of FLAG-TRPC3 in PrLs prepared from control nontransfected cells. Figure 1B,C shows $^{45}\text{Ca}^{2+}$ uptake in PrLs prepared from FLAG-TRPC3 IP fraction at extravesicular calcium concentrations of 25 μ M and 1 mM compared to that in control PrL prepared from nontransfected cells (note that $^{45}\text{Ca}^{2+}$ uptake into liposomes, i.e., prepared similarly but without protein, was also measured and subtracted from these values). Statistical analysis reveals a significant difference ($p < 0.05$, $n \geq 6$) between HEK and FLAG-TRPC3 PrLs at all time points in both cases. Similar PrL preparations from cells stably expressing FLAG-tagged TRPC3 with mutations of the conserved LFW motif (LFW to AAA) in the proposed pore-region of the protein resulted in substantially less $^{45}\text{Ca}^{2+}$ flux (Figure 1B,C) when compared to that seen in FLAG-TRPC3 PrLs. Statistical analysis reveals a significant difference ($p < 0.05$) between the FLAG-mut TRPC3 and FLAG-TRPC3 PrLs at >40 s. Uptake with the mutant protein containing PrL was not significantly different from that in control PrL from nontransfected HEK cells. This decrease in activity observed in the FLAG-mut TRPC3 cannot be explained by decreased amount of protein incorporated into the PrLs since similar reconstitutions (starting with equivalent

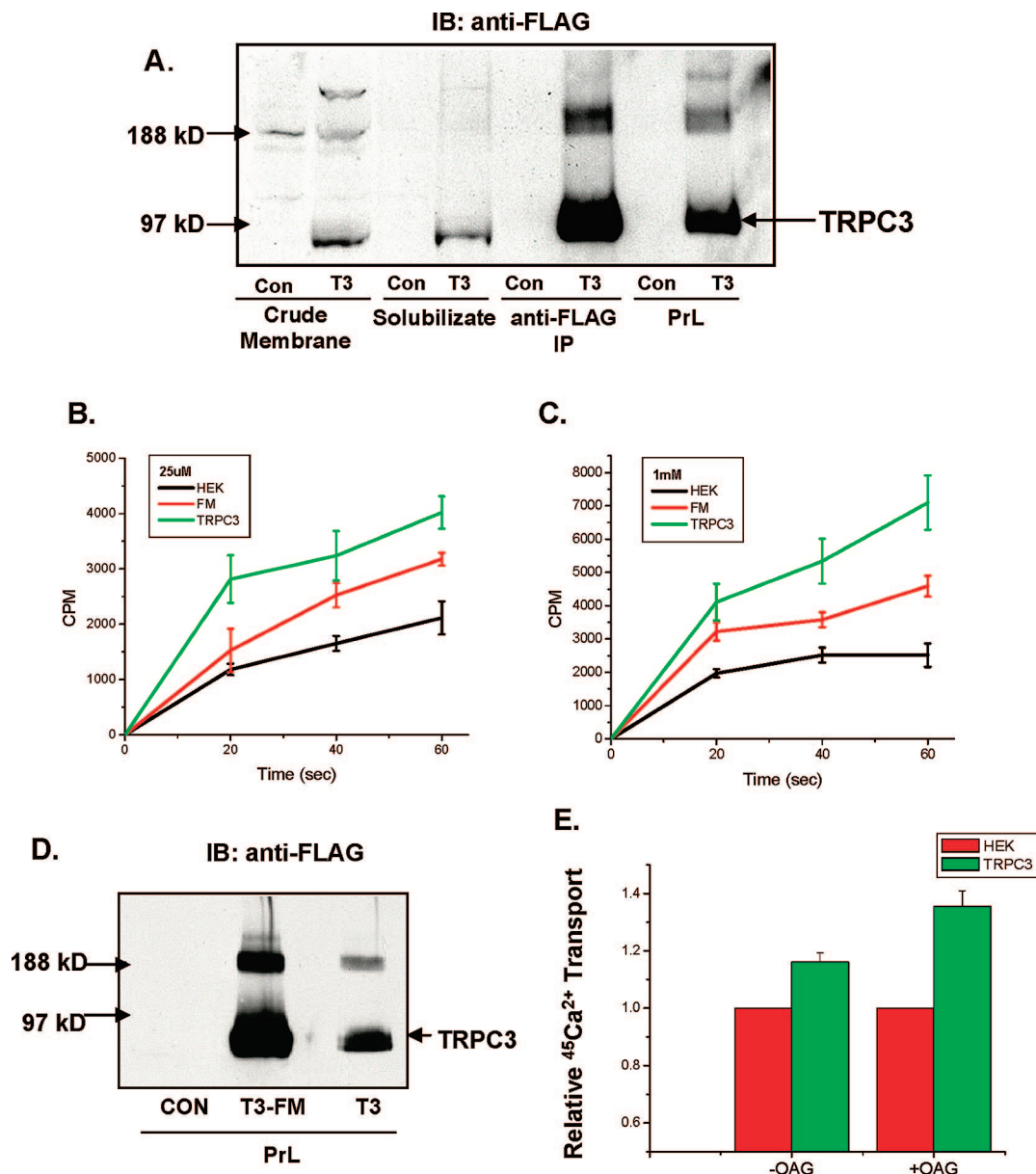


Figure 1. Ca²⁺ influx into HEK, FLAG-mut TRPC3, and FLAG-TRPC3-HEK proteoliposomes (PrLs). SDS-PAGE (using a 4–12% gel) on 50 mg of rat brain crude membrane and OG-extract from control (con) HEK and FLAG-TRPC3-HEK cells and 50 μL of anti-FLAG-IP and anti-FLAG-PrLs from control HEK or FLAG-TRPC3HEK cells was probed by Western blotting with anti-FLAG (panel A). Twenty-five microliters of either control HEK, FLAG-mut TRPC3, or FLAG-TRPC3-HEK PrLs was diluted to 250 μL into an assay medium consisting of 50 mM K-MOPS (pH 7.4), 200 mM KCl, and 1 mM MgCl₂ containing either 25 μM or 1 mM ⁴⁵CaCl₂. After 20, 40, and 60 s, duplicate 100 μL aliquots were removed, filtered, and counted as described in Experimental Procedures. To access the relative amounts of FLAG-mut TRPC3 and FLAG-TRPC3 incorporated into the PrLs, 25 μL of equivalent amounts of PrLs prepared from HEK, FLAG-mut TRPC3, and FLAG TRPC3 were analyzed by Western blotting (using anti-FLAG) and shown in panel D. After correcting for control liposomes, the uptake curves generated were plotted (mean ± SEM) in panels B and C. To determine if OAG (a DAG analogue) affected Ca²⁺ uptake, ±50 μM OAG was included in an assay medium containing 1 mM ⁴⁵CaCl₂. After 20 s, duplicate 100 μL samples were counted and relative increase in Ca²⁺ uptake (as compared to their respective HEK control PrLs) was plotted (mean ± SEM) in panel E.

amounts of extract) reveal greater amounts of protein incorporated into the FLAG-mut TRPC3 PrLs compared to the FLAG TRPC3 PrLs (Figure 1D). ⁴⁵Ca²⁺ transport into the FLAG TRPC3 PrLs was enhanced by the presence of 50 μM OAG (an analogue of diacylglycerol), a well-established known activator of TRPC3¹⁹ (Figure 1E). After correcting for control HEK PrL uptake, the amount of ⁴⁵Ca²⁺ transport into the FLAG TRPC3 PrLs in the presence of OAG was significantly higher ($p = 0.011$) as compared to levels observed in FLAG TRPC3 PrLs without OAG after 20 s in the presence of 1 mM Ca²⁺. These data

demonstrate that the conditions for solubilization and immunoprecipitation used here yield a functionally relevant preparation of TRPC3.

Solubilization and Immunoprecipitation of Native TRPC3 from Rat Brain. To determine the identity of proteins interacting with native TRPC3, rat brain crude membrane preparation was used to solubilize and immunoprecipitate the protein. A rabbit anti-TRPC3 polyclonal antibody¹⁰ was used to obtain the TRPC3-IP, while rabbit IgG was used to obtain a control immunoprecipitate (control-IP) which served as a

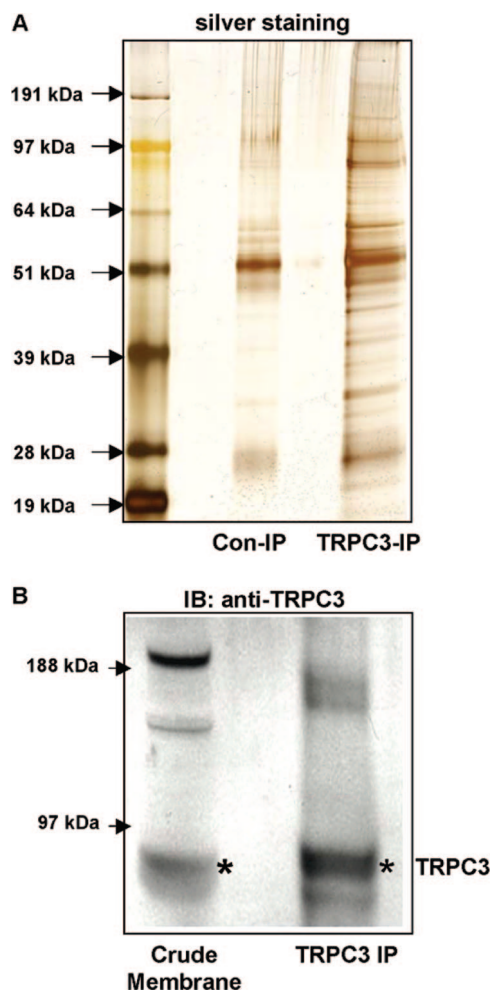


Figure 2. Immunoprecipitation of control rabbit IgG and TRPC3. (A) Proteins immunoprecipitated from solubilized rat brain crude membrane using rabbit IgG or anti-TRPC3 were separated (on 8% SDS-PAGE gels) and silver-stained. (B) To verify that TRPC3 was being immunoprecipitated, 50 μ g of rat brain crude membrane and 50 μ L of the TRPC3 IP fraction were separated on 8% SDS-PAGE gels, transferred to PVDF membranes, and then immunoblotted with anti-TRPC3. The band corresponding to TRPC3 as seen in panel B was not observed in the rabbit IgG IP fraction (data not shown).

control for nonspecific protein binding. Figure 2A shows the silver-stained gel of the TRPC3-IP fraction. A number of proteins can be visibly detected in this fraction which are not seen in control IP. Figure 2B shows the presence of TRPC3 in the TRPC3-IP fraction. On the basis of the presence of TRPC3 as well as other proteins, gels similar to that shown in Figure 2 were used for obtaining the samples for MS/MS analysis.

Identification of TRPC3-Interacting Proteins. In this study, we have used data obtained from two TRPC3-IP preparations and one rabbit IgG control immunoprecipitate. Specific databases and programs used to identify proteins with a high degree of confidence based on the peptide sequences are described in Experimental Procedures and summarized in Supplemental Tables 1 and 2 in Supporting Information. Figure 3 summarizes our evaluation strategy to assign a candidate protein as a specific TRPC3-interacting protein (Note that although it is quite possible that a number of these proteins might not actually directly interact with the channel, for simplicity, we have used the term interacting to describe the proteins specif-

ically detected in the TRPC3-IP). Briefly, the candidate protein satisfied one of the following criteria. (1) The candidate protein has two or more sibling peptides (multi-hit) to conclusively identify it, and it is present only in both TRPC3-IPs. (2) Multi-hit proteins appearing in both the TRPC3-IP and control IgG-IP (which also had one or more shared peptides that could be used for quantitative assessment) which demonstrated at least a 2-fold quantitative increase between TRPC3-IP and control-IP levels. (3) Proteins detected by single peptide identifications were assigned as a TRPC3-interacting protein only if additional biochemical verification (e.g., Western blotting) could confirm the presence of the protein. In all cases, the existence of at least one unique (distinct) peptide that could only be in the candidate's protein sequence was required. Searching of rat protein databases resulted in the identification of 64 proteins associated with TRPC3 (listed in Table 1). While all these TRPC3-interacting proteins have not been functionally characterized, previously reported studies have demonstrated that several of them directly interact with TRPC3 and regulate its function while several others have been reported to co-IP with TRPC3. We also have identified novel proteins which have not yet been described to have a role in TRPC3 function or regulation. Table 1 does not include protein identifications derived from procedural artifacts and/or contamination, for example, immunoglobins, trypsin, and keratins. An inherent shortcoming of antibody-based affinity purification studies is that the presence of more abundant IgG heavy and light chains obscure detection of less abundant protein species in their respective molecular weight ranges.

Validation of TRPC-Accessory Proteins by Western Blotting. Additional biochemical verification (i.e., Western blotting) was performed to support as many of the MS/MS identifications as possible. In the case of proteins identified only in the TRPC3-IP (not present in the control), a simple confirmatory Western blot was sufficient. Examples of these types of biochemical confirmations are shown in Figure 4A,B, which confirm the presence of neuromodulin (Figure 4A) and clathrin heavy chain (Figure 4B) in the TRPC3 immunoprecipitate. In order to use biochemical verification methods to confirm the quantifiable difference between proteins identified in both the TRPC3 and control IgG immunoprecipitates, equal amounts of control-IP and TRPC3-IP fractions (as determined by heavy/light chain bands quantification on SDS-PAGE gels) were analyzed. For example, panels C and D in Figure 4 reveal that for both Na^+/K^+ -ATPase and ANTI1, respectively, significantly greater amounts of both proteins are present in the TRPC3-IP than in the control-IP. Although an effort was made to verify as many of the proteins as possible, various factors prevented a confirmation of all of them (e.g., antibody not available).

Cellular Localization and Function of TRPC3-Associated Proteins. The 64 proteins identified as TRPC3-interacting proteins were grouped according to cellular location and function as revealed by the pie charts shown in Figure 5. Figure 5A reveals a wide variety of cellular locations in which the 64 TRPC3-interacting proteins are located, reflective of the many known or proposed interactions of TRPC3 with various organelles and structures within the cell. For example, plasma membrane components identified include previously reported Gq_α and plasma membrane SNAREs; ER proteins such as SERCA and IP3Rs; and vesicle trafficking proteins such as VAMP2. Of these, IP3Rs as well as SNARE proteins have been confirmed to be directly interacting with TRPC3 and regulating

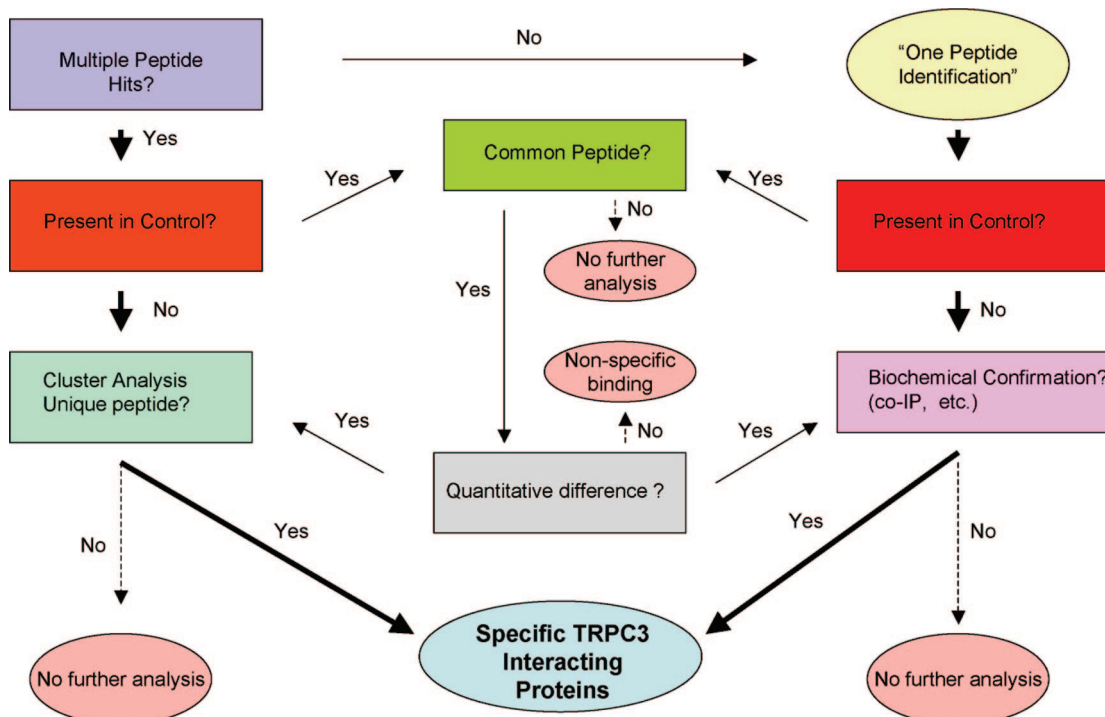


Figure 3. Flowchart of considerations in deciding if a protein identified in the TRPC3-IP is a “specific TRPC3 binding protein”. “Multiple Peptide Hit” proteins were distinguished from “One Peptide Identification” proteins by DBParser reports which assigned peptides to individual proteins. Common peptides (needed for quantitative analysis) were also derived from the DBParser reports. To determine the uniqueness of the peptides assigned to the identified proteins, cluster analysis using Mass Sieve was performed. Only proteins with unique peptides were considered for designation as a “specific TRPC3 interacting protein”.

channel function and trafficking, respectively.^{2,5} In Figure 5B, the 64 TRPC3-interacting proteins have been assigned into groups based on their cellular function. Again, a wide variety of functional groups are represented reflective of previously described mechanisms, such as vesicle fusion and trafficking as well as calcium signaling, that affect TRPC3 channel function. In addition, we identify a group of proteins which are localized in neuronal growth cones and have been shown to be associated with neuronal growth. Although TRPC3 has been shown to have a role in neuronal growth,²⁰ an association of these proteins with TRPC3 has not been described previously. Thus, these latter findings are important in future studies to understand the mechanism by which TRPC3 regulates the growth of neuronal cells.

Discussion

This study represents the first global, high-throughput proteomic analysis of native TRPC3 channel from rat brain. Since we have analyzed a native ion channel complex obtained by immunoprecipitation, nonspecific interactions typically associated with overexpressed epitope-tagged TRPC3 protein can be excluded. In our experience, immunoprecipitation and proteomic analysis of overexpressed FLAG-tagged TRPC3 resulted in the pull down of many proteins involved in protein synthesis and glycosylation (these findings are not presented here) which somewhat obscured the relatively lower abundant physiologically relevant proteins. In contrast, more physiologically relevant proteins, many of which have already been validated to have a role in TRPC3 function, were identified in the present study. Importantly, we show that the conditions used to solubilize and isolate TRPC3 allow recovery of the protein in a functionally active state as revealed by the higher Ca^{2+} flux

activity in PrLs containing TRPC3-IP as compared to those without FLAG-TRPC3 or containing mut-TRPC3. Additionally, Ca^{2+} influx into FLAG-TRPC3 PrLs, but not control PrL from nontransfected HEK cells, was increased by OAG, an analogue of DAG, which is a well-established activator of TRPC3.¹⁹ We suggest that the Ca^{2+} flux in TRPC3-containing PrL reflects the spontaneous activity associated with overexpressed TRPC3²¹ which is increased by OAG. These initial studies established conditions for immunoprecipitating native TRPC3 from rat brain which was then used for MS/MS analysis.

Sixty-four specific TRPC3-interacting proteins (see Table 1) were identified based on the criteria described in Figure 3. Table 2 lists some of the proteins which have been biochemically or functionally linked to TRPC3 previously, but were also detected on the basis of a single unique peptide (complete list of proteins can be found in Supplemental Tables 1 and 2 in Supporting Information). Although just one unique peptide is significant and can be used to confirm identification,²² these proteins have not yet been included in the specific TRPC3 proteome since further confirmation of their interaction or role in TRPC3 function is needed. Table 3 lists proteins which were identified by multiple peptides in the TRPC3-IPs but were also detected in control-IPs. These proteins have also not yet been included in the TRPC3 proteome because no common peptide was present, and thus, quantitative assessment of their presence in the TRPC3-IP could not be made. Further studies will be required to confirm whether these are accessory TRPC3 proteins. The 64 proteins which met our criteria for specific binding to TRPC3 have been assigned into groups based on their (1) cellular localization and (2) function. It is significant that a large number of these proteins have been previously shown to functionally and/or biochemically interact with

Table 1. TRPC3-Associated Proteins

entry name	protein ^a
Ca²⁺-Entry and Signaling	
1433B_RAT	14-3-3 family of phospho-Ser/Thr-binding proteins
1433E_RAT	
1433F_RAT	
1433T_RAT	
AT1A1_RAT	*Sodium/potassium-transporting ATPase α-1 and α-2 chain precursors, α-3 chain
AT1A2_RAT	
AT1A3_RAT	
AT2A2_RAT	*SR/ER calcium ATPase 2 (SERCA2)
AT2B1_RAT	*Plasma membrane calcium-transporting ATPases 1,2,3,4 (PMCA's 1,2,3,4)
AT2B2_RAT	
AT2B3_RAT	
AT2B4_RAT	
CSK11_RAT	Caskin-1 (CASK-interacting)
EAA1_RAT	Na ⁺ -dependent Glu/Asp transporters 1 and 2
EAA2_RAT	
GNAQ_RAT	Guanine nucleotide-binding protein
GNAZ_RAT	*G(q) and G(z) alpha subunits
ITPR1_RAT	*Inositol 1,4,5-trisphosphate receptor type 1
PEBP1_RAT	Phosphatidylethanolamine-binding protein 1 (PEBP-1)
RAP1A_RAT	Ras-related protein Rap-1A and Rap-1b precursors
RAP1B_RAT	
TENR_RAT	Tenascin-R precursor (TN-R) (Restrictin)
Associated with Neural Growth	
BASP_RAT	Brain acid soluble protein 1 (Neuronal axonal membrane protein NAP-22)
DPYL2_RAT	Dihydropyrimidinase-related protein 2 (DRP-2)
NCAM1_RAT	Neural cell adhesion molecule 1 (N-CAM 140)
NEUM_RAT	*Neuromodulin (Axonal membrane protein GAP-43)
NFASC_RAT	Neurofascin precursor
Associated with Vesicle Fusion	
SNP25_RAT	Synaptosomal-associated protein 25 (SNAP-25)
STX1A_RAT	Syntaxin-1A (Synaptotagmin-associated 35 kDa protein)
SV2A_RAT	Synaptic vesicle glycoprotein 2A (Synaptic vesicle protein 2A)
SYN1_RAT	Synapsin-1 (Synapsin I)
SYT1_RAT	*Synaptotagmin-1
TERA_RAT	Transitional endoplasmic reticulum ATPase (TER ATPase)
VAMP2_RAT	Vesicle-associated membrane protein 2 (VAMP-2) (Synaptobrevin-2)
Associated with Mitochondria	
ACON_RAT	Aconitate hydratase, mitochondrial precursor
ADT1_RAT	*ADP/ATP translocase 1 (ANT 1)
ATPB_RAT	ATP synthase subunit beta, mitochondrial precursor
CISY_RAT	Citrate synthase, mitochondrial precursor
COX2_RAT	Cytochrome c oxidase subunits 2 and 5A precursor
COX5A_RAT	
DHE3_RAT	Glutamate dehydrogenase 1, mitochondrial precursor (GDH)
FUMH_RAT	Fumarate hydratase, mitochondrial precursor (Fumarase)
IDH3B_RAT	Isocitrate dehydrogenase [NAD] subunit beta, mitochondrial precursor
LETM1_RAT	Leucine zipper-EF-hand-containing transmembrane protein 1, mitochondrial precursor
MDHC_RAT	Malate dehydrogenase, cytoplasmic and mitochondrial precursor
MDHM_RAT	

Table 1. Continued

entry name	protein ^a
SODM_RAT	Superoxide dismutase [Mn], mitochondrial precursor
VDAC1_RAT	Voltage-dependent anion-selective channel proteins 1 and 3 (VDAC-1 and *3)
VDAC3_RAT	
Associated with Endocytosis	
AP2A2_RAT	AP-2 complex subunits alpha-2 and beta-1
AP2B1_RAT	
CLH_RAT	*Clathrin heavy chain
DNM1L_RAT	Dynamin-1-like protein (Dynamin-like protein)
Miscellaneous	
ALDOC_RAT	Fructose-bisphosphate aldolase C
ANXA5_RAT	Annexin A5
DYHC_RAT	*Dynein heavy chain, cytosolic (DYHC)
FINC_RAT	Fibronectin precursor
KPYM_RAT	Pyruvate kinase isozymes M1/M2 (Pyruvate kinase muscle isozyme)
MAP2_RAT	Microtubule-associated protein 2 (MAP 2)
MYH10_RAT	Myosin-10 (Myosin heavy chain, nonmuscle IIb)
OXRP_RAT	150 kDa oxygen-regulated protein precursor (Orp150)
PGK1_RAT	Phosphoglycerate kinase 1
UCHL1_RAT	Ubiquitin carboxyl-terminal hydrolase isozyme L1 (UCH-L1)
VATB2_RAT	Vacuolar ATP synthase subunit B, brain isoform

^a Asterisk (*) represents confirmed by Western blotting.

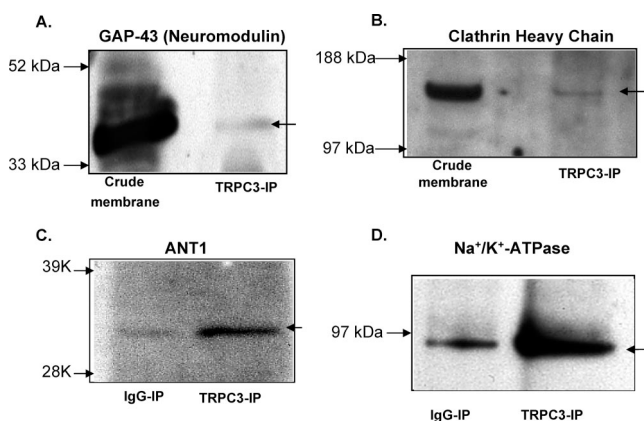


Figure 4. Western blot validation of MS/MS results. To confirm the presence of proteins identified only in the TRPC3-IP fraction by MS/MS, 50 μg of rat brain crude membrane and 50 μL of the TRPC3-IP fraction were separated on 8% SDS-PAGE gels, transferred to PVDF membranes, and then immunoblotted with the suspected protein. A positive confirmation revealed the presence of the suspect protein in the TRPC3-IP fraction (panels A and B). To confirm the quantitative difference in proteins identified in both the control rabbit IgG and TRPC3-IP fractions, equal amounts of immunoprecipitates (as determined by heavy and light chain presence) were immunoblotted as above (panels C and D). A positive confirmation resulted when at least a 2-fold increase in the suspected protein was observed in the TRPC3-IP fraction as compared to the control rabbit IgG (as determined by density scanning).

TRPC3. In particular, several of the known signaling proteins involved in PLC-mediated Ca²⁺ entry such as IP₃R1, SERCA2, and Gq_α, were identified in the TRPC3-specific group. Additional Ca²⁺ signaling proteins previously associated with TRPC3 such as PLCβ2, Homer 1, PKCβ, and alpha-2A adrenergic receptor were detected in addition to several proteins

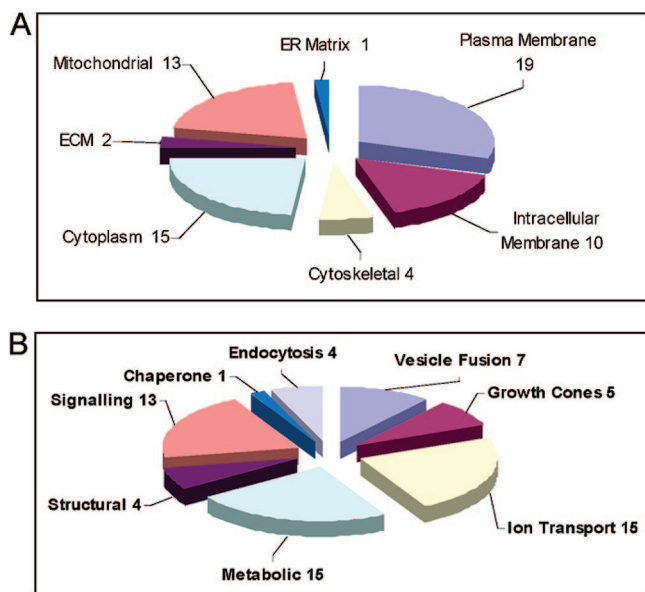


Figure 5. Cellular location and function of TRPC3-interacting proteins. Classification of TRPC3-interacting proteins are shown according to cellular location (panel A) and functional classification (panel B).

Table 2. Selected list of Relevant One-Hit Proteins

Calcium Entry and Signaling	
ADA2A_RAT ^a	Alpha-2A adrenergic receptor
HOME1_RAT ^b	Homer protein homologue 1
PLCB2_RAT ^c	Phospholipase C-beta-2
KPCB_RAT ^d	Protein kinase C beta type
CALR_RAT	Calreticulin precursor
CALX_RAT	Calnexin precursor
Associated with Vesicle Fusion	
SNAA_RAT	Alpha-soluble NSF attachment protein (SNAP-alpha)
SV2B_RAT	Synaptic vesicle glycoprotein 2B
RAB3A_RAT	Ras-related protein Rab-3A
RTN1_RAT	Reticulon-1 (Neuroendocrine-specific protein)
Associated with Neural Growth	
DREB_RAT ^e	Drebrin (Developmentally regulated brain protein)
SYNPO_RAT	Synaptopodin
CHIN_RAT	N-chimaerin (NC) (N-chimerin)
Glutamate Signaling	
GRIA2_RAT	Glutamate receptor 2 precursor (GluR-2)
GHC2_RAT	Mitochondrial glutamate carrier 2 (GC-2)
Associated with Endocytosis	
AMPH_RAT	Amphiphysin
AP180_RAT	Clathrin coat assembly protein AP180
RAB7_RAT	Ras-related protein Rab-7

^aPreviously linked to TRPC activity.⁴³ ^bShown to interact with TRPC3.⁴⁴ ^cShown to interact with TRPC3.¹⁰ ^dPreviously linked to TRPC3 activity.⁴⁵ ^eShown to interact with TRPC channels.²⁶

which have been previously linked to agonist-stimulated Ca²⁺ entry, for example, Na⁺/K⁺-ATPase and PMCA.^{23,24} Several ER proteins such as calnexin and calreticulin were identified which have been previously linked to IP₃ and ryanodine receptors and are likely to be important in intracellular calcium mobilization.²⁵ In a recent proteomic study using immunoprecipitated complexes of native TRPC5 and TRPC6²⁶ where selective regions of the gel were analyzed, a partial list of interacting proteins was identified. Interestingly, many of the proteins we

Table 3. Multi-Hit Proteins with No Common Peptide in Control

1433G_RAT	14-3-3 protein gamma
1433Z_RAT	14-3-3 protein zeta/delta
DHSA_RAT	Succinate dehydrogenase [ubiquinone]
COF1_RAT	Cofilin-1
MPCP_RAT	Phosphate carrier protein, mitochondrial precursor
ODPB_RAT	Pyruvate dehydrogenase E1 component subunit beta
OPA1_RAT	Dynamin-like 120 kDa protein, mitochondrial precursor
PYC_RAT	Pyruvate carboxylase, mitochondrial precursor
SPTA2_RAT	Spectrin alpha chain, brain
SPTN2_RAT	Spectrin beta chain, brain 2
THIL_RAT	Acetyl-CoA acetyltransferase, mitochondrial precursor
VPP1_RAT	Vacuolar proton translocating ATPase 116 kDa subunit a isoform 1
VDAC2_RAT	Voltage-dependent anion-selective channel protein 2

have identified here (e.g., Na⁺/K⁺-ATPase, endocytic vesicle-associated proteins clathrin, adapter-related protein complex AP-2, and a dynamin-1 like protein) were also reported in that previous study. Two other proteins, spectrin and actin, detected previously for TRPC5 and TRPC6, were also detected for TRPC3. However, these two proteins also appeared in our control IP; actin had a common peptide in both the control and TRPC3 IP which did not yield a quantifiable difference, while spectrin (despite many peptides identified) did not have a common peptide we could use to quantitatively assess the presence of the protein in the TRPC3-IP. Based on this, we have not designated either actin or spectrin as specific TRPC3-binding proteins.

Novel proteins that we have detected here include proteins associated with endocytosis, for example, clathrin assembly protein AP180, amphiphysin, and Ras-related protein Rab-7. Additionally, a dynamin-like protein and vacuolar proton translocating ATPase were also identified but not confirmed as unique to TRPC3 proteome since these were also present in control-IPs and no common peptides were present for determining quantitative differences. Collectively, presence of these endocytotic proteins suggests that TRPC3 is likely internalized via a clathrin-dependent pathway. We have previously described an exocytotic mechanism involved in recruitment and regulation of TRPC3 expression in the surface membrane⁵ mediated by members of the SNARE complex, such as VAMP2 and plasma membrane SNARE proteins, such as, syntaxin.²⁷ While confirming these previous findings, the present data reveal the putative molecular basis for TRPC3 trafficking; exocytosis, via a SNARE complex; and endocytosis, via clathrin-coated pits.

Other functionally relevant TRPC3-accessory proteins include several family members of the 14-3-3 proteins. The 14-3-3 family of proteins have been implicated a wide variety of cellular signaling processes.²⁸ Among the roles of the 14-3-3 family of proteins is PKC inhibition,²⁹ which is noteworthy since TRPC3 has been previously shown to be regulated by phosphorylation by PKC and PKG.³⁰ The 14-3-3 family of proteins are known to form homo- and heterodimers³¹ perhaps explaining our identification of several of the 14-3-3 family members in the TRPC3-IP. Since 14-3-3 proteins also serve as adaptor proteins, it is tempting to speculate that these interactions

between the phosphorylated TRPC3 and the 14-3-3 proteins could somehow explain the downstream effects of TRPC3 activation and deactivation. 14-3-3 proteins have also been shown to interact with various Ca^{2+} signaling proteins, including a number of G-protein coupled receptors and RGS proteins.³² Other proteins identified in the TRPC3 immunocomplex which could have possible implications in Ca^{2+} signaling include Caskin-1, a scaffolding protein which binds CASK, a calmodulin kinase domain containing protein. Since calmodulin has been previously shown to bind all of the TRPC channels and regulate several of the TRPCs,² perhaps the close proximity of a calmodulin kinase (CASK via Caskin-1) could have implications in regulation of TRPC3 function or of calmodulin-dependent regulation of downstream signaling events regulated via TRPC3-mediated Ca^{2+} signaling. Presently, there is little information regarding either of these mechanisms. Thus, the candidate proteins identified in the present study might provide useful targets to the physiological function of TRPC3-signaling pathway.

Mitochondria have been known to play a role in calcium entry by acting as a Ca^{2+} buffer which can result in greater store depletion and sensitivity to IP_3 .³³ A subset of mitochondria close to the plasma membrane (peripheral mitochondria) are thought to modulate Ca^{2+} entry by acting as a " Ca^{2+} sink" to reduce the ambient $[\text{Ca}^{2+}]$ which would otherwise exert feedback inhibition of Ca^{2+} entry.⁸ Additionally, the peripheral mitochondria provide a local source of ATP for the function of plasma membrane and ER pumps, for example, PMCA, SERCA, or even $\text{Na}^+/\text{K}^+/\text{ATPase}$.⁸ Consistent with these observations, we have identified a sizable number of mitochondrial proteins in the TRPC3 immunocomplex. Although physical or functional interactions between TRPC3 and mitochondria have not yet been established in the literature, our findings could be potentially important. For example, a recently proposed mechanism of mitochondrial modulation of Ca^{2+} entry is the release of mitochondrial agents such as glutamate³⁴ and ATP,³⁵ and one of the mitochondrial proteins we have identified is the precursor for glutamate dehydrogenase (Table 1), which increases the turnover of glutamate and has been implicated in learning and memory. Another potentially interesting candidate (with regards to glutamate regulation) is GC-2, a glutamate carrier protein from mitochondria. Additionally, we have linked TRPC3 to several mitochondrial transporters which could be involved in attenuating Ca^{2+} entry via ATP transport (ADP/ATP translocase 1) or by supplying counter-ion transport (members of the VDAC family of ion transporters). While these associations need to be validated by further biochemical and functional assays, it is interesting to speculate that TRPC3 function might be regulated by mitochondria localized in close proximity to the channel. Close functional association between mitochondria and a TRPC3-interacting protein, IP_3R (or ER) has been shown.³⁶ Thus, it is possible that scaffold proteins hold the IP_3R , mitochondria, and TRPC3 in a functionally coupled complex. Many of the mitochondrial proteins identified in the TRPC3 immunocomplex are enzymes associated with energy metabolism. Although it is unclear why TRPC3 and enzymes associated with energy metabolism in mitochondria are closely associated, it is interesting to note that the Ca^{2+} entry is affected by the energy state of the mitochondria. For example, several recent studies have implicated that ADP-ribose (ADPR) (a mitochondrial product from oxidative and nitrosative stress) can regulate Ca^{2+} entry into cells through certain TRP

family members.³⁷ Clearly, the modulatory effects on Ca^{2+} entry by mitochondria needs to be explored further.

A key finding was the presence of several proteins that are involved in neural growth cones.³⁸ Intracellular Ca^{2+} has been shown to play an essential role in growth cone extension and morphology as shown by the inhibition of growth cone motility and extension when plasma membrane calcium channels are blocked (even when activator of neural growth cones such as netrin-1 is present).³⁹ A recent study has shown that when endogenous TRPC3 expression is knocked out using siRNA, growth cone attraction in the presence of brain-derived neurotrophic factor (BDNF) is abolished.²⁰ In contrast, activation of TRPC5 by several growth factors induces an inhibitory effect on the extension of neural growth cones.⁴⁰ We have identified several proteins in the TRPC3-IP that have been implicated in neural growth (e.g., N-CAM 140 and neuromodulin) which is consistent with the proposed role of TRPC3 channels in neural growth. We also identified drebrin, which was also reported to be associated with TRPC5 and TRPC6.²⁶ It is tempting to speculate that the role of TRPC3 in neural growth cones is due to vesicle fusion events within the cell, as has been suggested for TRPC5.⁴⁰ TRPC5-vesicles fuse in a selective manner to the plasma membrane to regulate neurite extension.⁴¹ We have previously shown that TRPC3 incorporates into the plasma membrane from intracellular vesicles after stimulation of the cell.⁵ Confirming this, we have identified a number of key proteins involved in vesicular trafficking in the TRPC3-IP. Our previous hypothesis is that vesicle fusion to the plasma membrane is an important mechanism of regulation of TRPC3 expression in the plasma membrane and thus of Ca^{2+} entry function. Whether TRPC3-containing vesicles also carry critical cargo involved in neuronal growth is a concept that needs to be further investigated.

In summary, we present here a list of potential proteins in a native TRPC3 channel complex from rat brain. To our knowledge, this is the first report of TRPC channel proteome using a shotgun approach. Previous studies of TRPC5 and TRPC6 proteome used only selected regions of the gels for analysis. Our study reveals 64 potential TRPC3-specific accessory proteins. Some of these proteins have been previously shown by us and others to be involved in various aspects of TRPC3 function such as calcium signaling, exocytosis, and neural growth. Thus, the presence of these in the TRPC3-proteome has already been validated by functional and biochemical data. Additionally, we have identified novel protein interactions that suggest mechanisms for TRPC3 endocytosis via a clathrin-dependent pathway as well as possible regulation of channel function by mitochondria. With the use of such a shotgun approach where all the proteins associated with the target protein are identified, a sizable group of seemingly random proteins, albeit specific based on the selection criteria, can also appear as interacting proteins (Table 1-miscellaneous proteins). However, these were included in the TRPC3 proteome because this approach is unbiased and discovery-based as opposed to hypothesis-based. For example, a metabolic enzyme such as pyruvate kinase (Table 1) would appear to be unrelated to TRPC3 function. However, it is now evident that many traditional metabolic enzymes associate with proteins involved in ion transport. Although this has not been previously demonstrated for the TRP family of transporters, several glycolytic enzymes are components of the K(ATP) channel and regulate its function.⁴² It is important to recognize that TRPC3 isolated using a different approach or from a different tissue

might contain a different set of proteins, although some core proteins might be common. Further studies are required to determine which of the proteins we have identified are directly interacting with TRPC3 and to understand the function of these proteins and how they are assembled in the TRPC3 channel complex.

Supporting Information Available: Tables showing the specific databases and programs used to identify proteins with a high degree of confidence based on the peptide sequences. This material is available free of charge via the Internet at <http://pubs.acs.org>.

References

- Montell, C. J. *Physiol.* **2005**, *567*, 45–51.
- Kiselyov, K.; Kim, J. Y.; Zeng, W.; Muallem, S. *Pflugers Arch.* **2005**, *451*, 116–124.
- Ambudkar, I. S.; Ong, H. L. *Pflugers Arch.* **2007**, *455*, 187–200.
- Venkatachalam, K.; van Rossum, D. B.; Patterson, R. L.; Ma, H. T.; Gill, D. L. *Nat. Cell Biol.* **2002**, *4* (11), E263–272.
- Singh, B. B.; Lockwich, T. P.; Bandyopadhyay, B. C.; Lui, X.; Bollimuntha, S.; Brazer, S. C.; Combs, C.; Das, S.; Leenders, A. G.; Sheng, Z. H.; Knepper, M. A.; Ambudkar, S. V.; Ambudkar, I. S. *Mol. Cell* **2004**, *15*, 635–646.
- Lockwich, T. P.; Liu, X.; Singh, B. B.; Jadlowiec, J.; Weiland, S.; Ambudkar, I. S. *J. Biol. Chem.* **2000**, *275*, 11934–11942.
- Delmas, P.; Wanaverbecq, N.; Abogadie, F. C.; Mistry, M.; Brown, D. A. *Neuron* **2002**, *34*, 209–220.
- Park, M. K.; Ashby, M. C.; Erdemli, G.; Peterson, O. H.; Tepikin, A. V. *EMBO J.* **2001**, *20*, 1863–1874.
- Eder, P.; Poteser, M.; Groschner, K. *Handb. Exp. Pharmacol.* **2007**, *179*, 77–92.
- Bandyopadhyay, B. C.; Swaim, W. D.; Lui, X.; Redman, R. S.; Patterson, R. L.; Ambudkar, I. S. *J. Biol. Chem.* **2005**, *280*, 12908–12916.
- Lui, X.; Singh, B. B.; Ambudkar, I. S. *J. Biol. Chem.* **2003**, *278*, 11337–11343.
- Lockwich, T.; Singh, B. B.; Lui, X.; Ambudkar, I. S. *J. Biol. Chem.* **2001**, *276*, 42401–42408.
- Masuda, J.; Maynard, D. M.; Nishimura, M.; Ueda, T.; Kowalak, J. A.; Markey, S. P. *J. Chromatogr., A* **2005**, *106*, 57–69.
- Perkins, D. N.; Pappin, D. J.; Creasy, D. M.; Cottrell, J. S. *Electrophoresis* **1999**, *20*, 3551–3567.
- Bairoch, A.; Apweiler, R.; Wu, C. H.; Barker, W. C.; Boeckmann, B.; Ferro, S.; Gasteiger, E.; Huang, H.; Lopez, R.; Magrane, M.; Martin, M. J.; Natale, D. A.; O'Donovan, C.; Redaschi, N.; Yeh, L. S. *Nucleic Acids Res.* **2005**, *33*, D154–159.
- Yang, X.; Dondeti, V.; Dezube, R.; Maynard, D. M.; Geer, L. Y.; Epstein, J.; Chen, X.; Markey, S. P.; Kowalak, J. A. *J. Proteome Res.* **2004**, *3*, 1002–1008.
- McFarland, M. A.; Yang, X.; Makusky, A. J.; Geer, L. Y.; Kowalak, J. A.; Markey, S. P. Manuscript in preparation, **2007**.
- Slotta, D. J., et al. Manuscript in preparation, **2007**.
- Hofmann, T.; Obukhov, A. G.; Schaefer, M.; Gudermann, T.; Schultz, G. *Nature* **1999**, *397*, 259–263.
- Li, Y.; Jia, Y.-C.; Cui, K.; Zheng, Z.-Y.; Wang, Y.-Z.; Yuan, X.-B. *Nature* **2005**, *434*, 894–898.
- Vazquez, G.; Wedel, B. J.; Trebak, M.; St. John Bird, G.; Putney, J. W., Jr. *J. Biol. Chem.* **2003**, *278*, 21649–21654.
- Eng, J. K.; McCormack, A. L.; Yates, J. R., III. *J. Am. Soc. Mass Spectrom.* **1994**, *5*, 976–989.
- Hartford, A. K.; Messer, M. L.; Moseley, A. E.; Lingrel, J. B.; Delamere, N. A. *Glia.* **2004**, *45*, 229–237.
- Bautista, D. M.; Lewis, R. S. *J. Physiol.* **2004**, *556*, 805–817.
- Balaker, H.; Dziak, E.; Sojecki, A.; Librach, C.; Michalak, M.; Opas, M. *Hum. Reprod.* **2002**, *17*, 2938–2947.
- Goel, M.; Sinkins, W.; Keightley, A.; Kinter, M.; Schilling, W. P. *Pflugers Arch.* **2005**, *451*, 87–98.
- Singh, B. B.; Lockwich, T. P.; Bandyopadhyay, B. C.; Liu, X.; Bollimuntha, S.; Brazer, S. C.; Combs, C.; Das, S.; Leenders, A. G.; Sheng, Z. H.; Knepper, M. A.; Ambudkar, S. V.; Ambudkar, I. S. *Mol. Cell* **2004**, *15*, 635–646.
- van Heusdan, G. P. *IUBMB Life* **2005**, *57*, 623–629.
- Aitken, A.; Howell, S.; Jones, D.; Madrazo, J.; Martin, H.; Patel, Y.; Robinson, K. *Mol. Cell. Biochem.* **1995**, *149–150*, 41–49.
- Yao, X.; Kwan, H.-Y.; Huang, Y. *Neurosignals* **2005**, *14*, 273–280.
- Darling, D. L.; Yingling, J.; Wynshaw-Boris, A. *Curr. Top. Dev. Biol.* **2005**, *68*, 281–315.
- Abramow-Newerly, M.; Roy, A. A.; Nunn, C.; Chidiac, P. *Cell. Signalling* **2006**, *18*, 579–591.
- Parekh, A.; Putney, J. W. *Physiol. Rev.* **2005**, *85*, 757–810.
- Maechler, P.; Wollheim, C. *Nature* **2000**, *402*, 685–689.
- Landolfi, B.; Cursi, S.; Debellis, L. T.; Hofer, A. M. *J. Cell Biol.* **1998**, *142*, 1235–1243.
- Rizzuto, R.; Duchen, M. R.; Pozzan, T. *Sci. STKE* **2004**, *2004* (215), re1.
- Perraud, A. L.; Fleig, A.; Dunn, C. A.; Bagley, L. A.; Launay, P.; Schmitz, C.; Stokes, A. J.; Zhu, Q.; Bessman, M. J.; Penner, R.; Kinet, J. P.; Scharenberg, A. M. *Nature* **2001**, *411*, 595–599.
- Hong, K.; Nishiyama, M.; Henley, J.; Tessier-Lavigne, M.; Poo, M. M. *Nature* **2000**, *403*, 93–98.
- Mattson, M. P.; Kater, S. B. *J. Neurosci.* **1987**, *7*, 4034–4043.
- Ramsey, I. S.; Delling, M.; Clapham, D. E. *Annu. Rev. Physiol.* **2006**, *68*, 619–647.
- Craig, A. M.; Wyborski, R. J.; Banker, G. *Nature* **1995**, *375*, 592–594.
- Chowdhury, P. D.; Harrell, M. D.; Han, S. Y.; Jankowska, D.; Parachuru, L.; Morrissey, A.; Srivastava, S.; Liu, W.; Malester, B.; Yoshida, H.; Coetzee, W. A. *J. Biol. Chem.* **2005**, *280*, 38464–38470.
- Hill, A. J.; Hinton, J. M.; Cheng, H.; Gao, Z.; Bates, D. O.; Hancox, J. C.; Langton, P. D.; James, A. F. *Cell Calcium* **2006**, *40*, 29–40.
- Kim, J. Y.; Zeng, W.; Kiselyov, K.; Yuan, J. P.; Dehoff, M. H.; Mikoshiba, K.; Worley, P. F.; Muallem, S. *J. Biol. Chem.* **2006**, *281*, 32540–32549.
- Trebak, M.; Hempel, N.; Wedel, B. J.; Smyth, J. T.; Bird, G. S. J.; Putney, J. W., Jr. *Mol. Pharmacol.* **2005**, *67*, 558–563.

PR070496K